Conference Paper, Published Version

Nepf, Heidi; Zong, L.; Rominger, J.

Flow, deposition, and erosion near finite patches of vegetation

River Flow 2010 - Dittrich, Koll, Aberle & Geisenhainer (eds) - © 2010 Bundesanstalt für Wasserbau ISBN 978-3-939230-00-7

Flow, deposition, and erosion near finite patches of vegetation

H. Nepf, L. Zong, and J. Rominger
Massachusetts Institute of Technology, Cambridge, MA, USA

ABSTRACT: Laboratory and field-scale experiments reveal patterns of flow and transport near finite patches of vegetation. A laboratory study was done in a 1.2-m wide channel with a 40-cm wide patch of vegetation located along the channel wall. For most conditions, the patch was a sink for particles, as expected from the diminished flow and turbulence measured within the patch. However, for some conditions the deposition within the patch was limited by the supply of particles to the patch. A field-scale study was conducted at Saint Anthony Falls Laboratory. A sand-bed stream was constructed within a 40-m by 20-m retired spillway. Point bars were established within each meander during the first flood. Vegetation was then added to one point bar and subsequent changes to flow and topography were monitored. The inner region of the bar accumulated sediment, but the outer 30% of the bar was rapidly eroded due to the flow acceleration associated with the flow divergence. The seminar draws on additional studies to build generalizations about the competing roles of erosion and deposition in and around finite patches of vegetation.

Keywords: Vegetation, Deposition, Erosion, Stream channels

1 INTRODUCTION

By producing additional hydrodynamic drag, patches of aquatic vegetation change the mean flow distribution, which in turn may influence the distribution of sediment. Vegetation reduces the local velocity and therefore the local bed shear stress, so that it creates conditions that favor deposition and buffer against re-suspension (Gacia and Duarte, 2000; Cotton et al., 2006; Widdows et al., 2008). Thus, vegetation can influence channel morphology. For example, Tal and Paola (2007) experimentally showed that single-thread channels are stabilized by vegetation. Further, finite patches of vegetation have been associated with enhanced bed elevation within the patch, attributed to particle retention, and sometimes with diminished bed elevation at the edges of the patch, attributed to flow diversion (Fonseca et al. 1983, Bouma et al. 2007). In addition to altering the bed morphology, the capture of particles within vegetation enhances the retention of organic matter, nutrients and heavy metals within a channel reach (e.g. Schultz et al., 2002; Brookshire and Dwire, 2003; Windham et al., 2003). This paper describes laboratory and field-scale experiments that explore the flow and transport near finite patches of vegetation.

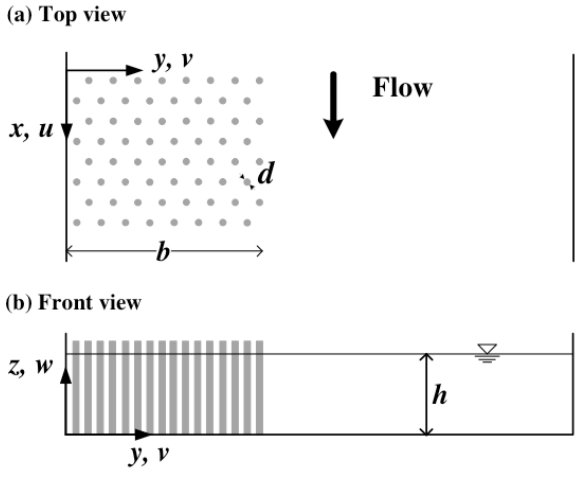

Figure 1. Schematic of laboratory study

2 LABORATORY STUDY

2.1 *Description of Flow Domain*

In this study we consider the deposition pattern within a finite region of bank vegetation. The model consists of an open channel partially filled

with emergent vegetation constructed from a staggered array of rigid circular cylinders (Figure 1). The cylinder array is described by the following parameters: the cylinder diameter, d, number of cylinders per unit bed area, n, the frontal area per unit volume, $a = nd$, and the average solid volume fraction of the array, $\phi = n(\pi d^2/4)$. We denote the stream-wise coordinate as x, with $x = 0$ at the leading edge of the vegetated region (Figure 2).

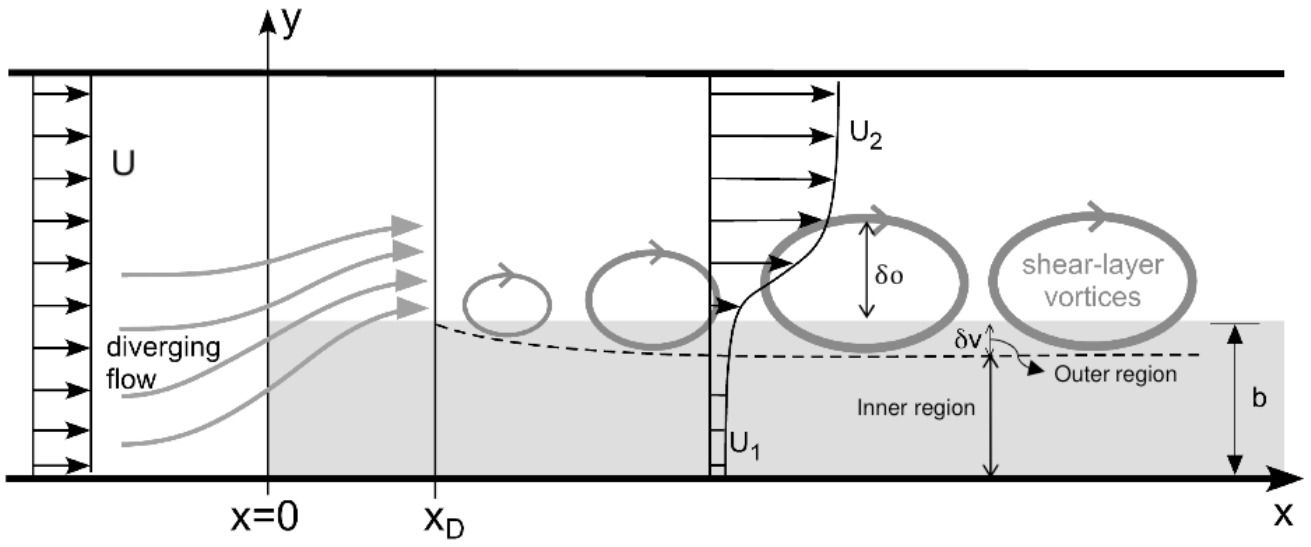

Figure 2. Top view of the flow near a finite patch of vegetation (grey) at the channel sidewall.

The lateral coordinate is y, with $y = 0$ at the side boundary. Because the vegetation creates high drag, much of the flow approaching the patch from upstream is diverted away from the patch. As show in Figure 2, the region of diversion begins upstream of and extends some distance into the vegetation (Zong and Nepf, 2010). The end of the flow diverging region is denoted by x_D. Beyond this point, the magnitude of the uniform flow within the patch (U_1) and in the open region (U_2) is set by the balance of potential gradient (due to bed and surface slopes) and the hydraulic resistance imposed by the stems and the bed. The difference between U_1 and U_2 creates a shear-layer at the interface between the parallel regions of emergent vegetation and open channel that in turn generates large coherent vortices via the Kelvin-Helmholtz instability, as also seen in free and shallow shear layers (*e.g.* Ho and Huerre, 1984; Chu et al., 1991). Similar structures form at the top interface of submerged vegetation (Ikeda and Kanazawa, 1996, Ghisalberti and Nepf, 2002). These energetic vortices dominate mass and momentum exchange between the vegetation and the adjacent open flow. The initial growth and the final scale of the vortices and their penetration into the patch, δ_v, are shown schematically in Figure 2. Based on laboratory experiment $\delta_v = 0.5(C_D\, a)^{-1}$, where C_D is the bulk drag coefficient for the vegetation (White and Nepf, 2007). If the patch width, b, is greater than the penetration scale, δ_v, the patch is segregated into an outer region of width δ_v that has rapid exchange with the adjacent open water and an inner region that has much slower exchange. The turbulent diffusivity, D_y, in outer region is ten to one hundred times higher, than that of the inner region (Ghisalberti and Nepf 2004, 2005).

The spatial distribution of deposition within the vegetation patch will depend on the flow conditions within the patch, as well as the delivery of particles to the patch. Particles can enter the patch from the leading edge ($x = 0$) through mean-flow advection, or from the lateral edge of the patch (y = b) through lateral dispersion. For flow depth h and settling velocity V_s, the settling time-scale, $T_s = h/V_s$, predicts the distance, x_a, over which particles entering from the leading edge advect before they are lost to deposition,

$$x_a = U_1 T_s = U_1 h/V_s \qquad (1)$$

Note that x_a is from the end of the flow diverging region (x_D).

For the particles entering the patch through lateral dispersion, the settling time scale, T_s, can also be used to estimate the maximum distance, δ_{max}, particles can be carried from the lateral edge.

$$\delta_{max} = 4\,(D_y h/V_s)^{1/2} \qquad (2)$$

If the patch length, l, is long enough ($l >> x_D + x_a$) and the width, b, is wide enough ($b > \delta_v + \delta_{max}$), there will be a region within the patch into which particles supplied from the upstream or from the

lateral edge cannot reach. If such regions exist within the patch, then the deposition within the patch will be supply limited.

2.2 *Experiment methods*

Experiments were conducted in a 16-m long recirculating flume with a test section that is 1.2-m wide and 13-m long. The flume was partially filled with a patch of model emergent vegetation, constructed with a staggered array of circular cylinders of diameter d = 6 mm. The patch was 0.4-m wide (1/3 of the flume width), 10-m long, and began 2 m from the start of the test section. The cylinders were held in place by perforated PVC baseboards that extended over the entire flume width. Two stem densities were considered, with a = 4 m^{-1} and 20 m^{-1}, corresponding to solid volume fractions of ϕ = 0.02 and 0.10, respectively. Three flow rates were tested for each patch density, with upstream channel velocities of U = 5 cm/s, 9 cm/s and 11 cm/s. The velocity field was measured using two Nortek Vectrino ADVs. A longitudinal transect was made through the centerline of the patch (y = 20cm), starting 2m upstream of the patch (x = -2m) and extending to the end of the patch (x = 10m).

Following the scale analysis done by Zong and Nepf (2010), we chose a model sediment of glass spheres with diameter d_P =12 μm and density ρ = 2500 kg/m^3 (Potters Industry, Inc., Valley Forge, PA), with a settling velocity on the order of V_s = 0.1mm/s. To begin the deposition study, 550g of particles were vigorously mixed across the width of the upstream feeder tank. The particles circulated with the water through the closed flow system. The net deposition was measured using rectangular microscope slides (75 mm × 25 mm), which were placed on the bed of the flume. The dry slides were weighed before placement. At the end of the experiment, the slides were baked overnight to remove moisture, and then reweighed. The weight of a slide after the experiment minus the weight before was taken as the net mass deposition. Three replicate experiments were made for each condition, and the uncertainty in net deposition was estimated from the standard error among replicates for each position.

2.3 *Results and Discussion*

The normalized velocity profiles collapsed into two groups, corresponding to the two patch densities (Figure 3). Approaching along the centerline of the patch (y = 20cm), the longitudinal velocity began to decrease one meter upstream of the leading edge for the dense patch (ϕ = 0.10) and 50 cm upstream of the leading edge for the sparse patch (Φ = 0.02). Within the patch (x > 0), the steamwise velocity continued to decrease until the diversion ended at roughly x_D = 200 cm for the dense patch and x_D = 300 cm for the sparse patch. Beyond the diverging region ($x > x_D$), the velocity within the vegetation was uniform ($\partial\bar{u}/\partial x$ = 0) until the end of the patch. The region $x > x_D$ will be called the fully developed region within the patch.

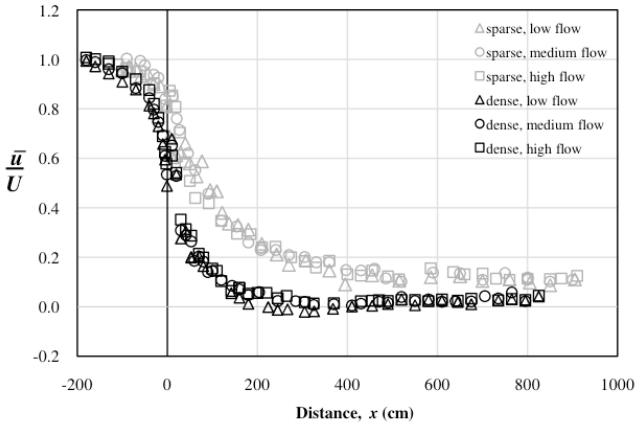

Figure 3. Normalized streamwise velocity along centerline of patch. Patch leading edge is at x = 0.

To illustrate the role of the advection distance, x_a, we consider the lateral patterns of deposition observed at positions both greater than and less than this distance (Figure 4). For each case, the deposition was normalized by the maximum deposition observed inside the patch, which was an approximation for the maximum potential deposition. We first consider the deposition pattern observed at comparable longitudinal positions (x = 700 and 735 cm), and at comparable channel speeds (U = 9 cm/s), but within patches of different stem density (Figure 4a). The difference in patch density produced different in-patch velocities, with U_I = 0.2 and 1.1 cm/s in the dense and sparse patch, respectively. This led to different advection distances, x_a = 260 cm (dense) and 1430 cm (sparse), which corresponded to different distances from the leading edge of $x_D + x_a$ = 460 cm (dense) and 1730 cm (sparse). For the sparse case, the position shown is less than $x_D + x_a$. This indicates that the particle supply is pre-dominantly by advection from upstream. Because the velocity is laterally uniform within the patch, the delivery is uniform, and the deposition within the patch is laterally uniform (Figure 4a). The deposition dropped near the flow edge (y = 36 cm) because of the enhanced turbulence associated with the shear-layer vortices. The diminished deposition (y = 36 cm) was within the region of vortex penetration, *i.e.* y = b -δ_v to $y = b$, which corresponded to y = 30 to 40 cm. for this case. In contrast, for the dense patch the deposition was not uniform across the patch width (Figure 4a). The deposition was

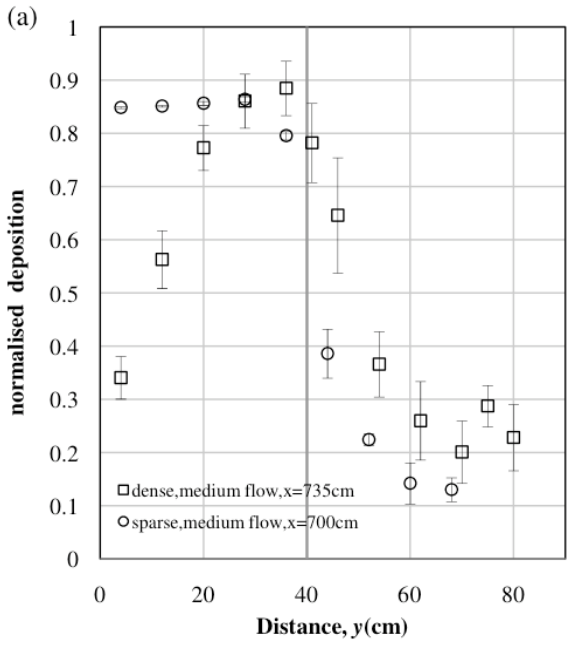

Figure 4a. Deposition in dense and sparse patch under the same flow conditions, U = 9 cm/s.

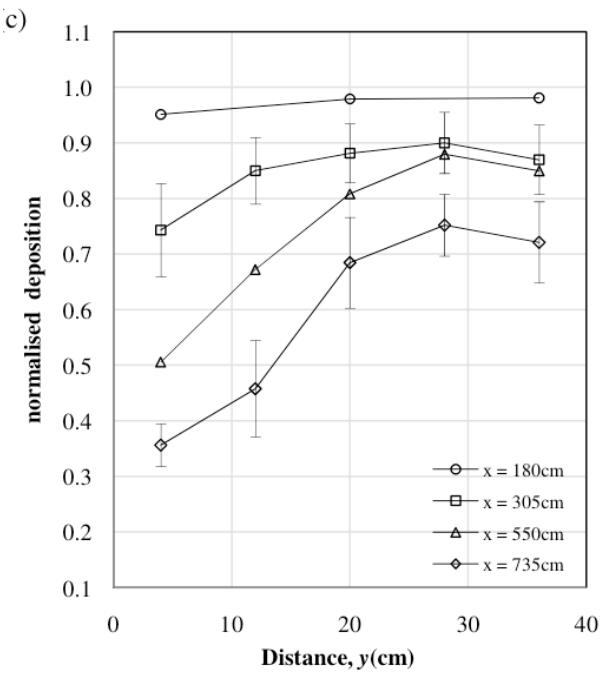

Figure 4c. Deposition in dense patch under high flow condition (U=5cm/s).

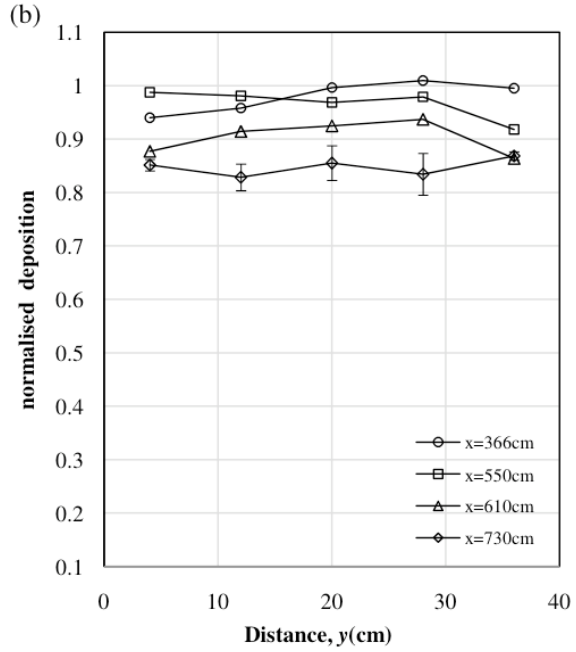

Figure 4b. Deposition in the sparse patch under low flow condition (U=5cm/s).

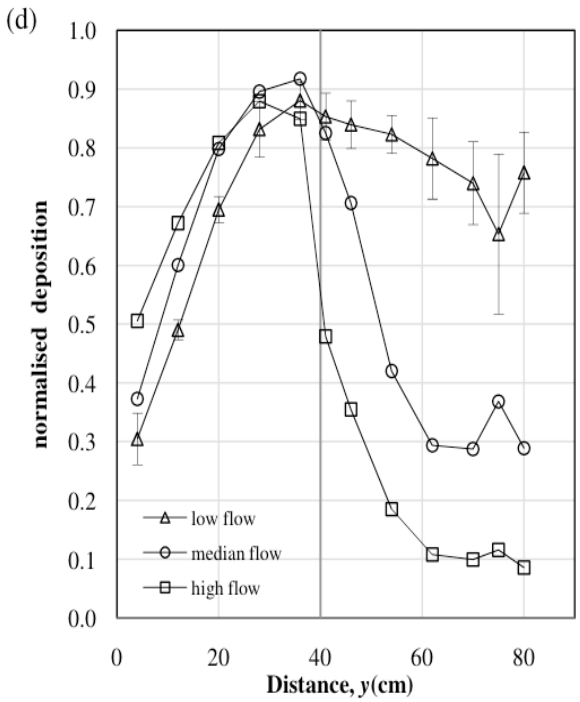

Figure 4d. Deposition measured at x = 550cm in the dense patch for three different flow conditions

highest near the flow-parallel edge (y = 40 cm) and decreased with the distance into the patch.

The pattern of deposition observed in the dense patch (Figure 4b) suggests that the supply of particles was by diffusion from the flow-parallel edge. For the dense patch (Figure 4a) the profile position (x) is greater than $x_D + x_a$ = 460cm, indicating that a significant fraction of the particles supplied from the leading edge had been lost upstream of this point, and the particles in this region of the patch are supplied pre-dominantly by diffusion from the flow-parallel edge. Indeed, the profile shape is similar to that observed by Sharpe and James (2006), who measured deposition under conditions for which the only source of particles to the vegetation patch was by diffusion from the flow-parallel edge.

We also considered how the lateral pattern of deposition evolved longitudinally within a single patch. We give two specific examples. For the sparse patch under the lowest channel flow (Figure 4b) the entire patch was shorter than the ad-

vection distance ($x_D + x_a$ = 11 m), and the deposition was uniform across the patch for the entire patch length. This is consistent with particle supply dominated by advection. The decline in deposition with increasing x can be attributed to the loss of suspended sediment to upstream deposition within the patch. In contrast, consider a case for which the total patch length was longer than the advection distance. In the dense patch with the highest flow, $x_D + x_a$ = 520cm. The deposition near the leading edge was laterally uniform (x = 180 cm). However, moving downstream, the deposition pattern gradually shifted to the signature shape of lateral flux ($x > x_D + x_a$).

Finally, the three deposition profiles measured in the dense patch, at the same position (x =550cm), but under the three different flow conditions are shown in Figure 4d. For all cases shown in this figure $x > x_a+x_D$. Across the patch width the deposition pattern was similar for all flow conditions, with maximum deposition near the edge of the patch and low deposition near the sidewall. As the upstream channel flow, U, decreased, the deposition in the patch decreased only slightly, while the deposition in the open region increased significantly. The trend in the open region is consistent with net deposition limited by re-suspension. As the open channel velocity decreased, re-suspension decreased, and net deposition increased. Within the patch, however, the deposition was supply limited, with supply dominated by the lateral flux from the flow-parallel edge. The lateral footprint of deposition was similar for the three flow speeds, which suggests that the lateral flux was also similar. This is consistent with known scaling for turbulent diffusion within vegetation. Previous studies have shown that lateral diffusivity within vegetated regions scales as $D_y \sim U_1 d$ (Nepf et al. 2007). Together with (2), and the fact the stem diameter, d, is the same for all three cases, we expect that lateral footprint of deposition, δ_{max}, will be comparable for all flow cases, consistent with the observation.

2.4 *Conclusion*

Particles are supplied to a patch of vegetation by mean advection through the leading edge and by lateral turbulent diffusion through the flow-parallel edge. The relative contribution from these two sources is described by the length-scale, x_D+x_a. For $x < x_D+x_a$, the supply of suspended particles is dominated by mean advection and the net deposition is laterally uniform across the patch width. Beyond x_D+x_a the supply is dominated by lateral flux from the flow-parallel edge, and the net deposition is highest near that edge and decreasing toward the patch interior. If the length of the patch, L, is much longer than x_D+x_a, then there can be regions of the patch that will have limited deposition due to a lack of suspended particle supply. Cotton et al. (2006) include possible examples of the supply-limited condition in their observations of fine sediment deposition within patches of *Ranunculus*.

3 FIELD-SCALE STUDY

3.1 *Description of Facility and Methods*

A second set of experiments was conducted in the Outdoor StreamLab (OSL), an experimental facility built on a retired spillway adjacent to the University of Minnesota's St. Anthony Falls Laboratory in downtown Minneapolis. During 2008 a sand-bed stream was constructed with three meander bends that have an average wavelength of 25 m and a sinuosity of 1.3 (Figure 5).

The system can provide water discharges up to 2100 L/s, although flows for this set of experiments were considerably smaller. Through the summer of 2008, a base flow of 38 L/s was maintained in the stream. Bank-full flood events, representative of the average flood magnitude in natural channels, occurred at approximately weekly intervals, each lasting nine hours with a flow of 208 L/s. The banks of the channel were fixed in geometry and position with coconut fiber matting, but the bed of the channel was mobile, and consisted of coarse-grained sand (median grain size: D_{50} = 0.7 mm). A recirculating sediment system recycled bedload sediment lost from the downstream end back to the upstream end of the stream. During the first flood event, point bars formed from the mobile bed material near the inner bank of the meander bends. These point bars formed within the first few hours of the first flood event on July 10, 2008, and remained as stable artifacts during the base flow and subsequent flood events in summer 2008.

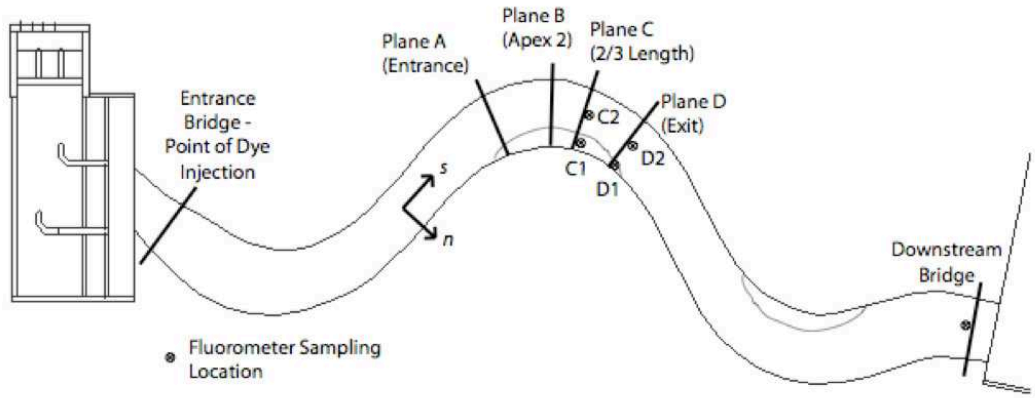

Figure 5. Top view of Outdoor StreamLab

Velocity measurements were made during each of the 9-hr flood events. A Nortek Vectrino Acoustic Doppler Velocimeter (ADV) was used to measure velocity at the cross sections shown in Figure 5. The ADV was mounted on a motorized traverse oriented perpendicular to the local stream direction. The velocity was recorded at each point for between 120 to 240 seconds at 25 Hz. Surveys using a Leica Total Station were used to gather geometric information about the channel geometry as it developed over the summer. Following the third flood, two reed species, *Juncus effusus* and *Scirpus atrovirens* were planted on the portion of the sand bar in the second meander that was exposed at base flow. This vegetation was planted in a staggered array that produced a vegetated frontal area per unit volume of $a = 5.2$ m^{-1}, where $a = nd_{plant}$, $n = 69$ m^{-2} is the number of plants per unit area, and $d_{plant\ (avg)} = 0.075$ m is the characteristic diameter of the plant.

3.2 *Results and Discussion*

As expected, a secondary circulation was observed in the meander bends prior to the addition of vegetation. The circulation was most intense near the apex of the meander, with a strong lateral outflow near the water surface and a return current near the bed of the stream (Figure 6b). The secondary circulation predominantly occupied the deeper part of the cross section, with smaller lateral, v, and vertical velocities, w, over the bare point bar. The depth-averaged streamwise velocity was highest near the outer bank of the meander and smallest over the point bar (Figure 6a).

During the first flood event after the planting, the cross-sectional geometry changed rapidly due to the flow disturbance created by the plants. The outermost row of plants was scoured away, as well as part of the next outermost row, removing approximately 50 cm of the point bar width along with most of the vegetation in this zone. This loss in point bar area, observed in the early stages of the flood, was confirmed by photographic and survey data. Similar measurements for the unvegetated point bar in meander 3 showed no loss in emergent bar area, confirming that the losses observed in the second point bar were due to the added vegetation. The plants that were not scoured away in the first hours of the first flood were stable for the remainder of the summer flood sequence.

Both the depth-averaged streamwise velocity and the secondary circulation at the apex of the meander changed significantly after the vegetation was added (Figure 7). The depth-averaged streamwise velocity decreased over the bar and increased in the open region (Figure 7a). In addition, the secondary circulation increased in strength, but was confined to the deepest section of the channel. Finally, over the point bar, a strong outwards (toward outer bank) flow now extended over the entire depth of the water column.

The difference in the velocity field before and after the addition of the vegetation occurred because the vegetatiVve drag decreased the flow over the bar, which created additional lateral diversion of flow toward the open channel. This diversion led to an acceleration of flow at the edge of the vegetation, causing the observed scour. Specifically, the velocity at the vegetation edge (y = 50 cm) increased from 45 cm/s before the addition of vegetation (Figure 6a) to 55 cm/s after the addition of vegetation (Figure 7a). In addition, after the vegetation was added, the centrifugal force

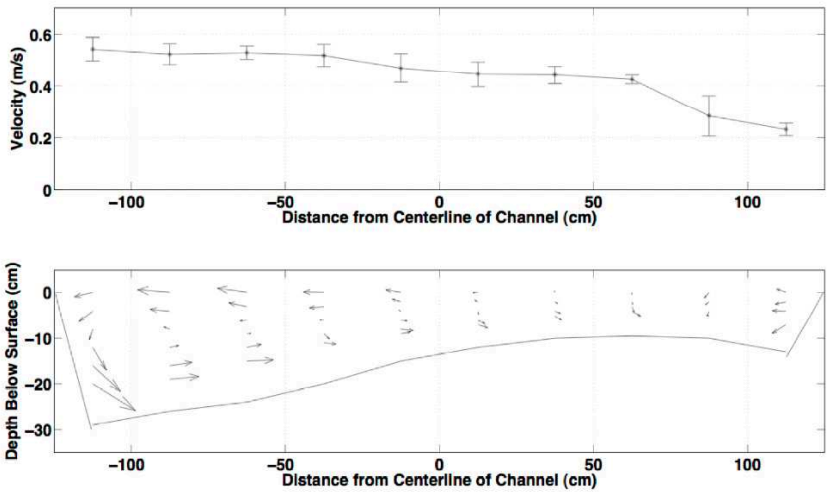

Figure 6. Velocity Measurements at Apex with bare point bar. (a) Depth averaged downstream velocity, and (b) velocity components in the lateral and vertical directions. The cross-sectional outline shows the measured bed profile.

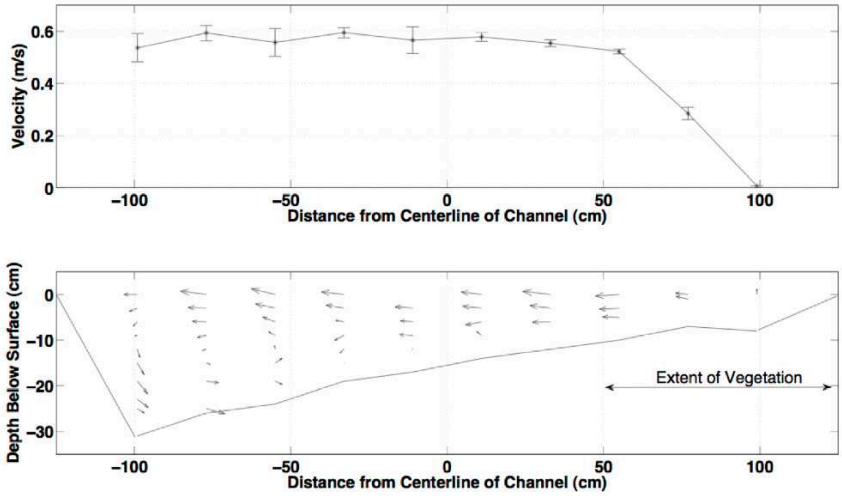

Figure 7. Velocity Measurements at Apex with vegetated point bar. (a) Depth averaged downstream velocity, and (b) velocity components in the lateral and vertical directions. The cross-sectional outline shows the measured bed profile

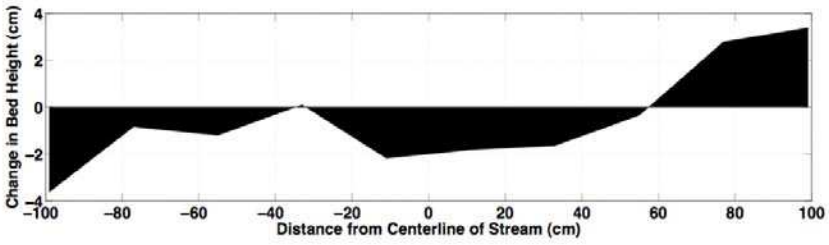

Figure 8. Change in bed elevation after the addition of vegetation measured at the meander apex.

exceeded the cross-stream pressure gradient over the entire depth over point bar, causing a lateral flow toward the open channel and outer bank that extended over the water depth in the vegetated region, *i.e.* there was no return flow at the bed (Figure 7b). The return current near the bed was limited to only the deepest parts of the channel, in contrast to the conditions before the vegetation (Figure 6b), in which the return flow extended onto the bar. This implies that the addition of vegetation changed the secondary flow in such a way as to cut off sediment supply from the open channel to the bar.

Measurements of the bed geometry taken before and after the vegetation was added show how the depth-profile changed (Figure 8). Approx-

imately 4 cm of sediment was deposited within the vegetation and 2 cm of erosion occurred at the edge of the vegetation. Bouma et al (2007) made similar observations near artificial islands of vegetation planted in a tidal flat. In that study two stem densities were considered. For patches with the higher stem density, significant erosion occurred at the edges of the newly planted vegetation, while deposition occurred within the patch, similar to the observations reported here. However, at the lower stem density only deposition within the patch was observed, with no significant erosion at the patch edge. This indicates the important role of stem density in setting the relative magnitudes of deposition and erosion generated by vegetation.

Finally, in the present study erosion also occurred in the deeper parts of the cross section near the outer bank. Recall that here the outer bank of the channel was protected from erosion by fiber matting. If the outer bank had not been protected, it would have likely experienced erosion, because the strength of the secondary circulation increased significantly with the addition of vegetation. In a natural channel, we anticipate that the vegetation addition would accelerate the growth of the inner bar while eroding the outer bank, and therefore might accelerate the growth of the meander.

3.3 *Summary*

In the second experiment, we showed that the addition of vegetation may promote erosion as well as deposition. Following the addition of vegetation, erosion occurred near the lateral edge of the new patch of vegetation, resulting in a 33% loss of emergent bar width at the apex. However, deposition occurred further into the vegetation, near the inner stream bank. The observations suggest that the spatial accelerations caused by the presence of the vegetation shifted the sand bar area to a new geometric equilibrium.

ACKNOWLEDGEMENTS

This material is based upon work supported by the US National Science Foundation under Grant EAR 0738352. Any opinions, conclusions or recommendations expressed in this material are those of the authors and do not necessarily reflect the views of the National Science Foundation. This project was also supported by a National Center for Earth-surface Dynamics (NCED) Visitor Program Grant.

REFERENCES

Bouma,T., van Duren,L., Temmerman,S., Claverie,T., Blanco-Garcia,A., Ysebaert,T., Herman,P., 2007. Spatial flow and sedimentation patterns within patches of epibenthic structures: Combining field, flume and modeling experiments. *Con. Shelf Res*, 27, 1020-1045

Brookshire, E.N.J., Dwire, K.A., 2003. Controls on patterns of coarse organic particle retention in headwater streams. J.N. Am. Benth. Soc. 22, 17–34.

Chu, V.H., Wu, J.-H., Khayat, R.E., 1991. Stability of transverse shear flows in shallow open channels. J. Hydr. Eng. 117, 1370–1388.

Cotton, J., Wharton, G., Bass, J., Heppell, C., Wotton, R., 2006. The effects of seasonal changes to in-stream vegetation cover on patterns of flow and accumulation of sediment. Geomorphology 77, 320–334.

Fonseca, M.S., Zieman, J.C., Thayer, G.W., Fisher, J.S., 1983. The role of current velocity in structuring eelgrass meadows. Est. Coast. Shelf Sci. 17, 367–380.

Gacia E, Duarte CM., 2000. Sediment retention by a merditerranean Posidonia oceanica meadow: The balance between deposition and resuspension. Est. Coast. Shelf. Sci., 52,505-514.

Ghisalberti, M., Nepf, H., 2002. Mixing layers and coherent structures in vegetated aquatic flow. JGR, 107, 10.1029/2001JC000871

Ghisalberti, M., Nepf, H., 2004. The limited growth of vegetated shear layers. Water Resour. Res. 40, W07502.

Ghisalberti, M, Nepf, H., 2005. Mass transfer in vegetated shear flows. Env. Fluid Mech. 5, 527–551.

Ho, C.M., Huerre, P., 1984. Perturbed free shear layers. Ann. Rev. Fluid. Mech., 16, 365–424.

Ikedam S., and M. Kanazawa, 1996. Three-dimensional organized vortices above flexible water plants. J. Hydraul. Eng., 122(11), 634-640.

Nepf, H., Ghisalberti, M., White, B., Murphy, E., 2007. Retention time and dispersion associated with submerged aquatic canopies. Water Res. Res, 43, W04422. doi:10.1029/2006WR005362

Schultz, M., Kozerski, H.-P., Pluntke, T., Rinke, K., 2002. The influence of macrophytes on sedimentation and nutrient retention in the lower River Spree (Germany). Water Res. Res., 37, 569–578.

Sharpe, R.G., and James, C.S., 2006. Deposition of sediment from suspension in emergent vegetation. Water SA, 32(2), 211-218.

Tal, M., Paola, C., 2007. Dynamic single-thread channels maintained by the interaction of flow and vegetation. Geology, 35, 347–350.

White, B., Nepf, H., 2007. Shear instability and coherent structures in a flow adjacent to a porous layer. J. Fluid Mech. 593, 1–32.

Windham, L.,Weis, J.S.,Weis, P., 2003. Uptake and distribution of metals in two dominant salt marsh macrophytes, Spartina alterniflora and Phragmites australis. Estuar. Coast. Shelf Sci. 56, 63–72.

Widdows, J., Pope, N.D., Brinsley, M.D., 2008. Effect of Spartina anglica stems on near-bed hydrodynamics, sediment erodability and morphological changes on an intertidal mudflat. Marine Ecology Progress series 362, 45-57.

Zong, L., Nepf, H.M., 2010. Flow and deposition in and around a finite patch of vegetation. *Geomorphology*, 116, 363-372